

Effects of BSS Corrosion Behavior on Neutron Absorption Performance in an Accelerated Environment in a Spent Nuclear Fuel Wet Storage

Daehyeon Park^a, Yunju Lee^a, Junhyuk Ham^a, Seung Chang Yoo^b, Kiyong Kim^c, Donghee Lee^c, Yongdeog Kim^c and Ji Hyun Kim^{a*}

^a Department of Nuclear Engineering, Colledge of Engineering, Ulsan National Institute of Science and Technology (UNIST), 50, UNIST-gil, Ulsan 44919, Republic of Korea

^b Korea institute of nuclear safety, 291, Daehak-ro, Yuseong-gu, Daejeon, Republic of Korea

^c Korea Hydro & Nuclear Power Corporation, 70, Yuseoung-daero 1312, Yuseong-gu, Daejeon 34101, Republic of Korea

*Corresponding author: kimjh@unist.ac.kr

1. Introduction

In several spent fuel pools(SFP), such as Kori unit 3 and Hanbit units 3 and 4, borated stainless steel (BSS) is used as the structural material for the spent fuel pool high-density storage rack to maintain the criticality of spent fuels. Since it is difficult to replace the storage rack, corrosion resistance and neutron absorbency are required for a long period.

BSS is based on stainless steel 304 and is specified in the ASTM A887-89 standard, depending on the boron concentration, ranging from 304B (0.20-0.29% B) to 304B7 (1.75-2.25% B) [1]. Boron has low solubility in austenitic stainless steel, so it creates a secondary phase of metallic borides like (Fe, Cr)₂B. A previous study reported that the Cr content difference between metallic borides and the substrate affects the short-term oxidation behavior of BSS [2,4]. However, the corrosion behavior of BSS in conditions similar to those found in SFPs is not fully understood, even though they contain high concentrations of dissolved oxygen and boron. Additionally, a long-term corrosion study has not been conducted for this material. For these reasons, an accelerated corrosion experiment was conducted in simulated SFP conditions to understand the long-term corrosion behavior of BSS. Additionally, the long-term integrity of the degraded BSS was assessed by analyzing its ability to absorb neutrons over time as it aged.

2. Methods and Results

2.1 Accelerated corrosion experiments condition

To simulate the long-term corrosion of BSS, an experiment at an accelerated temperature was planned since it is not possible to conduct a corrosion test for several decades. The operating environment of the SPF is 25°C with 4,200 ppm of boron ions and atmospheric air conditions. Even though it is an atmospheric air condition, the DO concentration, which affects the corrosion rate of BSS, is not measured during operation. In this experiment, it was assumed to be 2,000 ppb according to a previous study, which reports that the

oxidation behavior of stainless steel is maintained over 300 ppb [3].

Corrosion mechanisms are transformed if the system temperature is increased above a certain value. Previous studies show that corrosion of SS304 can occur equally below 250°C, and the corrosion activation energy of SS304 is proportional to temperature and inversely proportional to DO concentration in boric acid. The corrosion activation energy of SS304 in 2,000 ppb of DO and 250°C of boric acid is calculated to be 21.3 kJ/mol [4]. As explained in the above studies, the accelerated coefficient was 30 times according to the Arrhenius equation.

Thus, to simulate 0.5, 5, 10, 15, 20, 30, 45, and 60 years of corrosion in SFP, BSS specimens were exposed to 250°C, 2,000 ppb of DO concentration, and boric acid with 4,200 ppm of boron ions for 0.2, 2, 4, 6, 8, 12, 16, and 24 months.

2.2 Sample preparation

The chemical composition of the specimen used in this study is presented in Table 1. The specimen was cut into 20 mm × 20 mm × 3 mm with a 2 mm hole on one side, which was used to hang the specimen in an autoclave with Pt wire insulated with a zirconia sleeve. All specimens were polished with SiC paper up to 800 grits and then ultrasonically cleaned in deionized water.

Table I: Chemical composition of BSS [wt.%]

| Fe | B | Cr | Ni | C |
|------|------|-------|--------|------|
| Bal | 2.07 | 20.28 | 13.32 | 0.08 |
| Mn | Si | P | S | |
| 1.30 | 0.29 | 0.01 | 0.0003 | |

2.3 Analysis method

To investigate the microstructural characteristics of specimen, the ex-situ investigation was conducted using scanning electron microscope (SEM) coincidence with energy dispersive X-ray spectroscopy (EDS). To observe the cross section of specimens, focused ion beam (FIB)

was also used. Detailed chemical analysis was performed with electron probe X-ray micro analyzer (EPMA).

2.4 Morphology of oxidized specimen

Detailed results and discussion of as-received and earlier specimen were presented in previous study [5]. In summary, microstructure of BSS was composed of substrate and secondary phase, which was $(Fe, Cr)_2B$.

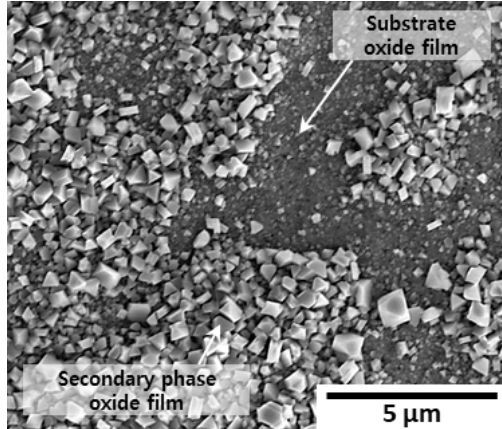


Figure 1 Surface SEM images of BSS specimens after 12 months of accelerated corrosion in high DO borated water

Figure 1 shows a secondary electron image of oxidized specimens that were exposed for 12 months. An oxide film formed on the BSS substrate in a polyhedral form on the surface of both the substrate and the secondary phase. In particular, the oxide on the secondary phase grew larger than that on the substrate. Additionally, the oxides were densely packed on the secondary phase particle compared to the substrate.

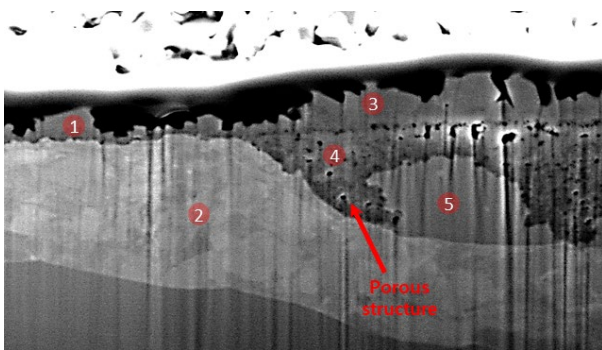


Figure 2 Cross section SEM images of BSS specimens after 12 months of accelerated corrosion in high DO borated water. EDS points were indicated in each image

Table II: Point EDS results of 12 months exposed specimen presented in figure 2

| Type | | O (at.%) | Fe (at.%) | Cr (at.%) | Ni (at.%) |
|-------------------------------|---|----------|-----------|-----------|-----------|
| Oxide film of substrate | 1 | 32.84 | 27.49 | 11.64 | 28.03 |
| Substrate | 2 | 8.11 | 53.52 | 25.69 | 12.68 |
| Oxide film of secondary phase | 3 | 40.51 | 21.79 | 12.86 | 24.85 |
| Oxidized secondary phase | 4 | 43.24 | 28.48 | 18.68 | 9.61 |
| Secondary phase | 5 | 8.02 | 25.57 | 63.63 | 2.79 |

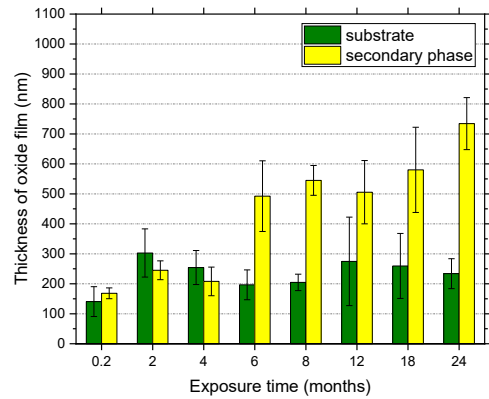


Figure 2 Oxide thickness change of substrate and secondary phase in BSS specimen

Figure 2 shows SEM images of the cross-section of specimens after an accelerated corrosion experiment for 12 months. As shown in the figure, the oxide layer formed on the substrate is thinner than that on the secondary phase. Also, secondary phases that were exposed to water were oxidized, as shown by the red arrow in Figure 2. The oxidized secondary phase has a porous structure.

The oxide film formed on the substrate and secondary phase is considered to be Fe_2O_3 , $NiFe_2O_4$, and Cr_2O_3 from EDS analysis, which are passivation layers formed in a high DO concentration environment of general stainless steel. As shown in Figure 3, the clear difference in oxide film thickness between the substrate and secondary phase after 6 months could indicate that the secondary phase is oxidized more.

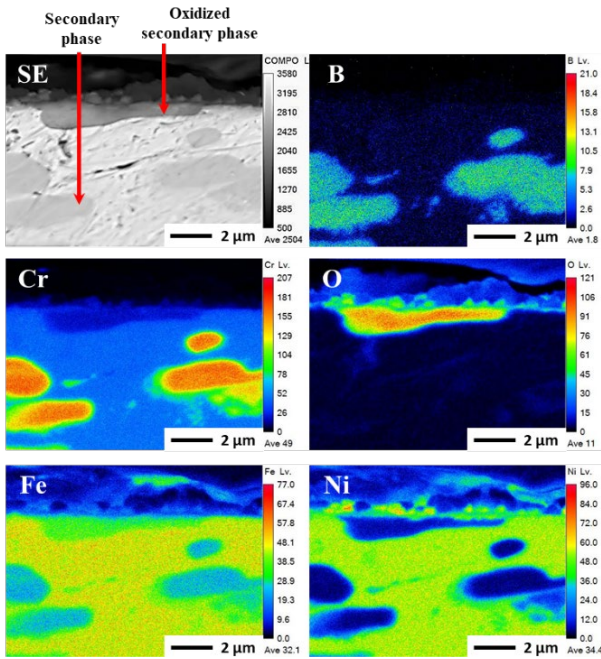


Figure 3 Cross section EPMA mapping images of BSS specimens after 12 months of accelerated corrosion in high DO borated water

In the accelerated corrosion experiment, cross-sectional specimens were analyzed using EPMA after 12 months. Figure 4 displays the results of this analysis, which revealed the chemical composition of Fe, Cr, Ni, B, and O. The figure indicates that the oxidized secondary phase has significantly lower concentration of B and Cr compared to the non-oxidized secondary phase. This could be because the oxidation of B and Cr has the lowest Gibbs free energy compared to other elements. Because oxidized B is highly soluble in water, it dissolves outside, and Cr forms an unstable oxidation state. As a result, the secondary phase is transformed into a porous structure, which leads to an increase in the diffusion rate of metal elements in the surrounding substrate.

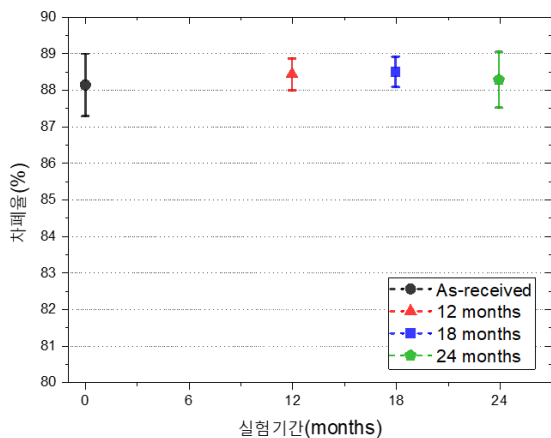


Figure 5 Change in shielding rate with accelerated corrosion experiment time

Using Boron's high cross section for neutrons, the neutron absorption performance of BSS was evaluated through neutron transmission tests. Figure 5 shows the effect of the corrosion behavior of BSS on its neutron absorption performance. Samples simulated to undergo up to 60 years of degradation before corrosion through accelerated corrosion testing did not show significant changes in the neutron shielding ability before and after corrosion. This can be explained in relation to the corrosion behavior of BSS. Boron was only leached out from the secondary phase exposed on the surface, and this oxidized secondary phase corresponds to about 0.17% of the volume of the total secondary phase. This can be seen as a very small proportion compared to the total boron content and is not expected to have a significant impact on neutron absorption performance.

3. Conclusions

To investigate the long-term corrosion behavior of BSS used as a structural material in SFP, an accelerated corrosion experiment was conducted, and subsequent analysis was carried out. The accelerated corrosion experiment was conducted for 0.2, 2, 4, 6, 8, 12, 16, and 24 months to simulate corrosion over 0.5, 5, 10, 15, 20, 30, 45, and 60 years.

The thickness of the oxide layer formed on the secondary phase increased faster than that on the substrate, and it was prominently observed after being exposed for 6 months. The secondary phase was also more oxidized than the substrate. From the Gibbs free energy of each oxidation reaction, it was determined that the oxidation of B had the lowest Gibbs free energy compared to other elements.

Oxidized B has a characteristic of being soluble in water, and oxidized secondary phase has a porous structure that serves as a diffusion path for metal elements in the surrounding substrate. It was found that an oxide film of secondary phase, which is thicker than the substrate oxide film, was formed in the secondary phase due to an increased diffusion rate.

Samples simulated to undergo up to 60 years of degradation before corrosion through accelerated corrosion testing did not show significant changes in the neutron shielding ability before and after corrosion.

ACKNOWLEDGEMENT

This work was financially supported by Korea Hydro & Nuclear Power Co., Ltd. This study contains the results obtained by using the equipment of UNIST Central Research Facilities (UCRF). This work was supported by the Nuclear Safety Research Program through the Korea Foundation Of Nuclear Safety(KoFONS) using the financial resource granted by the Nuclear Safety and Security Commission(NSSC) of the Republic of Korea. (No.2103084)

REFERENCES

- [1] ASTM International. "ASTM A887-89 (2004): Standard Specification for Borated Stainless Steel Plate, Sheet, and Strip for Nuclear Application." Published on CD-ROM. West Conshohocken, Pennsylvania: ASTM International. 2008.
- [2] Moreno, D.A.; Molina, B.; Ranninger, C.; Montero, F.; Izquierdo, J. Microstructural Characterization and Pitting Corrosion Behavior of UNS S30466 Borated Stainless Steel. *Corrosion* 2004, 60, 573–583.
- [4] Ha, Heon Young, Jae Hoon Jang, Tae Ho Lee, Chihyoung Won, Chang Hoon Lee, Joonoh Moon, and Chang Geun Lee. "Investigation of the Localized Corrosion and Passive Behavior of Type 304 Stainless Steels with 0.2-1.8 Wt % B." *Materials* 11, no. 11 (2018): 1–15.
- [4] Duan, Zhengang, Farzin Arjmand, Lefu Zhang, and Hiroaki Abe. "Investigation of the Corrosion Behavior of 304L and 316L Stainless Steels at High-Temperature Borated and Lithiated Water." *Journal of Nuclear Science and Technology* 53, no. 9 (2016): 1435–46.
- [5] Daehyeon Park, Yunju Lee, Junhyuk Ham, Seung Chang Yoo, Kiyoun Kim, Donghee Lee and Ji Hyun Kim "Corrosion Behavior of (Fe, Cr)₂B Metallic Boride of Borated Stainless Steel in Borated Water Environment" 2021 Transactions of the Korea Nuclear Society Fall Meeting.